

# THz Imaging Using Rail-based Synthetic Aperture Radar for the Detection of Concealed Objects

Syed An Nazmus Saqueb\*, Joseph L. Garry, Graeme E. Smith, Niru K. Nahar and Kubilay Sertel

Dept. of Electrical and Computer Engineering  
Electroscience Laboratory, The Ohio State University  
Columbus, OH 43212, USA

saqueb.1@osu.edu, garry.6@osu.edu, smith.8347@osu.edu, nahar.2@osu.edu, sertel.1@osu.edu

**Abstract**—We present, a rail-based synthetic aperture radar (SAR) imaging system for THz band. A 1-port full-duplex frequency extender coupled with a vector network analyzer was used as the transceiver module. Using a motorized linear stage, slanted object is scanned across the transmitter field of view and reflection is measured in frequency domain in two waveguide bands (220-325 GHz and 500-750 GHz). Processing the frequency data, images of metallic objects concealed in thick dielectric layers were reconstructed with resolution as fine as 0.8 mm.

## I. INTRODUCTION

Imaging in Terahertz (THz) band has attracted significant interest in recent years due to key features, such as their non-ionizing property and high spatial resolution. Albeit keen interest from the industry, proliferation of THz imaging is hindered by excessive cost and large size of the available imaging systems. Recently, single-pixel imaging based on compressive sensing and spatial light modulator implemented via photoexcitation of semiconductor showed promise to realizing low-cost, high resolution, real time THz imaging systems [1], [2]. This method relies on optically reconfigured masks to serialize the measurements, hence it is free of any motion. Nevertheless, this technique is better suited for small-scale applications where the imaging aperture dimension is smaller than few centimeters. It is quite difficult to implement compressive imaging for the detection of concealed objects inside large structures, such as walls, vehicles, and humans. Alternatively, synthetic aperture radar technique can be deployed to achieve a very large aperture by scanning the object in azimuth using a linear rail [3]. In this paper, we present a rail-based synthetic aperture radar (SAR) imaging system in WR3.4 (220-325 GHz) and WR1.5 (500-750 GHz) bands. We demonstrate a prototype using a vector network analyzer (VNA)-based measurement system and a motorized translation stage. We show that non-destructive imaging of objects through high-permittivity and thick dielectric materials is possible with resolution as fine as 0.8 mm.

## II. PROPOSED RAIL-BASED SAR IMAGING IN THZ BAND

Rail-based SAR, more commonly known as the strip-map SAR, synthesizes the numerical aperture by “dragging” the sensor’s beam across the imaging scene [4], [5]. The geometry of the proposed method is shown in Fig. 1. The transceiver is

placed on a linear rail to scan the object along its cross-range and with an inclined incidence angle for range resolution. This grazing angle, denoted as  $\phi$  in Fig. 1, is necessary to ensure the entire object is interrogated with the radiation and minimize object shadowing. For  $i$ th position on the rail, complex-valued reflection  $R_i$  is measured in the operating frequency band.

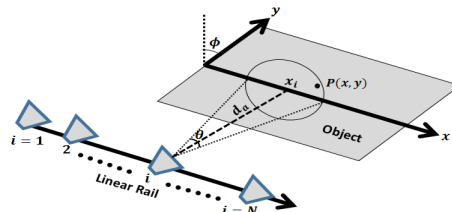


Fig. 1: Proposed rail-based SAR geometry where  $N$  successive reflection measurements are collected from a scene and subsequently processed to construct the object of interest.

To reconstruct any pixel  $P(x, y)$  on the scene, each frequency response  $R_i$  is first brought back to time response by adding a phase shift of  $2\pi f d_i(x, y)/c$ , where  $f$  is the frequency,  $d_i(x, y)$  is the distance between the pixel and the sensor at  $i$ th position in the rail and  $c$  is the speed of propagation in free space. After this simple phase compensation, the collected data is summed constructively to calculate the total response from the pixel  $P(x, y)$ . Finally to reconstruct the object of interest, all responses across the frequency band are summed up and the magnitude square of the complex value is taken as the pixel intensity. Thus, the intensity  $I(x, y)$  of pixel  $P(x, y)$  can be written as,

$$I(x, y) = \left| \sum_{f=f_1}^{f_2} \sum_{i=1}^N R_i e^{2\pi f d_i(x, y)/c} \right|^2 \quad (1)$$

where  $N$  is the number of sample points on the rail and  $f_2 - f_1$  is the instrument bandwidth. The distance  $d_i(x, y)$  can be calculated as

$$d_i(x, y) = \sqrt{(d_a + y \cos \phi)^2 + (y \sin \phi)^2 + (x_i - x)^2} \quad (2)$$

from the geometry where,  $d_a$  is the constant distance between rail axis and  $x$ -axis on the image and  $x_i$  is the azimuth position of the antenna for  $i$ th sample. The cross-range or  $x$ -resolution is,  $\delta_x = \frac{c}{4f \sin \frac{\phi}{2}}$ , where  $f$  is the center frequency of the radar

system and  $\theta$  is the antenna beam-width. Similarly, the down-range or  $y$ -resolution is,  $\delta_y = \frac{c}{2B \cos \phi}$ , where  $B$  is the effective bandwidth and  $\phi$  is the grazing angle [6].

### III. EXPERIMENTAL SETUP AND RESULTS

The experimental setup for THz SAR imaging system is illustrated in Fig. 2. We used a frequency extender manufactured by Virginia Diodes, which is then coupled with a Keysight's N5242A VNA (VNAx system) as radar transceiver. The 1-port full-duplex (transmit and receive) frequency extender modules consists of frequency multiplier chains that attach to the VNA and are used to up-convert the VNA LO frequency sweep (about 12GHz) to the desired mmW/THz bands (covering WR-8 to WR-1) spanning 90GHz up to 1.1THz. A conical

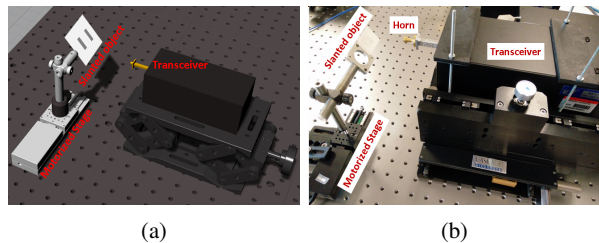


Fig. 2: VNA-based rail SAR system: (a) Computer model and (b) photograph of the experimental setup.

or diagonal horn antenna is used to couple the waveguide mode of the VNAx to free-space radiation to illuminate the scene under test. To achieve translation of the scene across the field of view of the horn, the object is mounted on a motor controlled translation stage (ThorLabs MTS50-Z8). For each step in the translation, complex reflection in full spectrum is collected and processed in MATLAB to reconstruct the image.

We first used a WR3.4 band (225-330 GHz) extender as the transceiver. In the two examples shown in Fig. 3,  $64 \times 64$ -pixel images were reconstructed for a  $1.2 \times 3.2 \text{ cm}^2$  area using 0.5 mm steps in azimuth scan. In both cases, the grazing angle was  $40^\circ$  and the horn beam-width was  $10^\circ$ , resulting in 3mm cross-range and 1.6mm of down-range ( $y$ ) resolution. Next, we considered two M6 screws placed behind a 0.2mm-thick paper using both WR3.4 (220-325 GHz) and WR1.5 (500-750 GHz) bands. The grazing angle and the horn beam-width were same for both bands. However, WR1.5 band produces images with 1.3 mm cross-range and 0.8 mm down-range resolution due to its higher center frequency and bandwidth. As seen in Fig. 4, WR1.5 band produces much finer image than WR3.4 band.

### IV. CONCLUSION

We present, a rail-based SAR imaging system in 220-325 GHz and 500-750 GHz bands. Using VNA-based measurement and a motorized linear stage, high resolution images of metallic objects inserted within thick dielectric slabs were reconstructed. The cross-range and down-range resolution in 500-750 GHz band were 1.3 mm and 0.8 mm respectively. Using WR1.0 (750-1100 GHz) band, this simple system can achieve a cross-range resolution of 0.9 mm and a down range resolution as small as 0.5 mm. The presented system

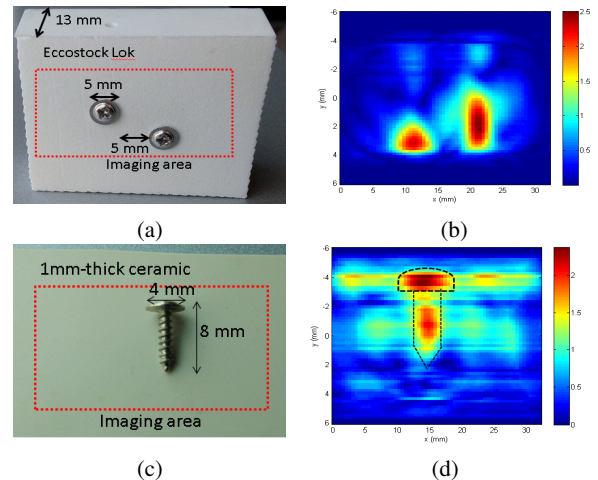


Fig. 3: (a) Two metallic screws are inserted on the back side of a thick dielectric layer (Eccostock LoK,  $\epsilon_r = 1.7$ ), (b) reconstructed SAR image, (c) a metallic screw is glued on the back side of a 1mm-thick layer of Barium-Strontium Titanate ( $\epsilon_r > 90$ ), and (d) reconstructed SAR image.

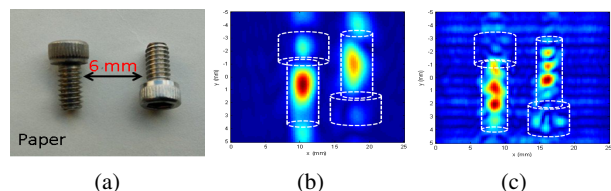


Fig. 4: (a) Two metallic (M6) screws behind a 0.2mm-thick paper. Reconstructed SAR image (b) using WR3.4 (220-325 GHz) band and (c) using WR1.5 (500-750 GHz) band.

can be used for non-destructive evaluation applications to detect impurities, cracks, rust, voids, etc. for a wide range of materials typically used in construction, such as drywall, wood, brick, concrete and cinder-block, to name a few.

### REFERENCES

- [1] D. Shrekenhamer, C. M. Watts, and W. J. Padilla, "Terahertz single pixel imaging with an optically controlled dynamic spatial light modulator," *Optics express*, vol. 21, no. 10, pp. 12507–12518, 2013.
- [2] A. Kannegulla, Z. Jiang, S. Rahman, M. Shams, P. Fay, H. Xing, L.-J. Cheng, and L. Liu, "Coded-aperture imaging using photo-induced reconfigurable aperture arrays for mapping terahertz beams," *IEEE Transactions on Terahertz Science and Technology*, vol. 4, no. 3, pp. 321–327, 2014.
- [3] J. T. Richard and H. O. Everitt, "Millimeter wave and terahertz synthetic aperture radar for locating metallic scatterers embedded in scattering media," *arXiv preprint arXiv:1701.02342*, 2017.
- [4] J. L. Garry, G. E. Smith, and C. J. Baker, "Practical implementation of stripmap doppler imaging," *IET Radar, Sonar & Navigation*, vol. 9, no. 8, pp. 974–983, 2015.
- [5] G. L. Charvat, L. C. Kempell, and C. Coleman, "A low-power high-sensitivity x-band rail sar imaging system [measurement's corner]," *IEEE Antennas and Propagation Magazine*, vol. 50, no. 3, pp. 108–115, 2008.
- [6] D. R. Wehner, "High resolution radar," *Norwood, MA, Artech House, Inc., 1987, 484 p.*, 1987.